



# Deposition of selenium thin layers on gold surfaces from sulphuric acid media: Studies using electrochemical quartz crystal microbalance, cyclic voltammetry and AFM

Murilo Feitosa Cabral<sup>a</sup>, Valber A. Pedrosa<sup>b,\*</sup>, Sergio Antonio Spinola Machado<sup>a</sup>

<sup>a</sup> Instituto de Química de São Carlos, Universidade de São Paulo, C.P. 780, 13566-590 São Carlos, SP, Brazil

<sup>b</sup> Department of Materials Engineering, Samuel Ginn College of Engineering, Auburn University, Auburn, AL 36849, USA

## ARTICLE INFO

### Article history:

Received 22 July 2009

Received in revised form

26 September 2009

Accepted 3 October 2009

Available online 13 October 2009

### Keywords:

Selenium

EQCM

Underpotential deposition

AFM

## ABSTRACT

In this paper we report here new considerations about the relationship between the mass and charge variations ( $m/z$  relationship) in underpotential deposition (UPD), bulk deposition and also in the  $H_2SeO_3$  formation reaction. Nanogravimetric experiments were able to show the adsorption of  $H_2SeO_3$  on the AuO surface prior to the voltammetric sweep and that, after the AuO reduction, 0.40 monolayer of  $H_2SeO_3$  remains adsorbed on the newly reduced Au surface, which was enough to give rise to the UPD layer. The UPD results indicate that the maximum coverage with  $Se_{ads}$  on polycrystalline gold surface corresponds to approximately 0.40 monolayer, in good agreement with charge density results. The cyclic voltammetry experiments demonstrated that the amount of bulk Se obtained during the potential scan to approximately 2 Se monolayers, which was further confirmed by electrochemical quartz crystal microbalance (EQCM) measurements that pointed out a mass variation corresponding of 3 monolayers of Se. In addition, the Se thin films were obtained by chronoamperometric experiments, where the Au electrode was polarized at +0.10 V during different times in 1.0 M  $H_2SO_4$  + 1.0 mM  $SeO_2$ . The topologic aspects of the electrodeposits were observed in Atomic Force Microscope (AFM) measurements. Finally, in highly negative potential polarizations, the  $H_2Se$  formation was analyzed by voltammetric and nanogravimetric measurements. These finding brings a new light on the selenium electrodeposition and point up to a proposed electrochemical model for molecule controlled surface engineering.

© 2009 Elsevier Ltd. All rights reserved.

## 1. Introduction

Over the past years, much research has been devoted to exploring the potential of semiconductors for future electronic devices. Therefore, development of new methods to control surface properties is an area of great interest. Recently, several inorganic compounds were extensively tested in order to obtain durable, uniform and compact metal coatings for semiconductor thin films prepared at constant room temperature and pressure conditions [1]. Among them, selenium deposition plays a distinctive role as one of the most practical technique to obtain precursor films to be doped for semiconducting layers in several applications.

For the purpose of surface modification, electrodeposition method has been shown to reduce costs remarkably when compared with most physical methods [2,3]. It was already known that the mechanical properties of electrodeposits are affected by the initial stages of the electrodeposition process [4]. Recently, therefore, researchers have used an underpotential deposition process

on several semiconductor substrates, which exhibit an intriguing thickness-dependent stability, because this phenomenon occurs at a potential more positive than the equilibrium potential [5]. Underpotential deposition (UPD) provides a straightforward approach for controllably and reproducibly modifying structure and composition of metal electrodes with a layer of dissimilar metal [6,7].

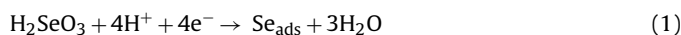
Moreover, the underpotential deposition has been applied in activating noble metals [8], formation of arrays of nanoparticles [9], deposition of chalcogenides using the electrochemical atomic layer epitaxy [10], and a template to characterize the formation of self-assembled layers [11,12].

Several investigators have used the quartz microbalance (EQCM), often in combination with cyclic voltammetric, with AFM of semiconductor films proving to be a powerful tool for conservation in situ and investigation of surface roughness effects during electrochemical metal depositions and dissolution [13–15]. Understanding such selenium special behavior in thin films growth is a major aim in several electrochemical studies.

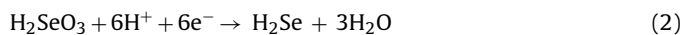
Selenium ad-atom deposit has been the focus of a large body of research [16–22]. The electrochemical reduction of  $Se^{4+}$  in aqueous solutions is a complex subject, which has been studied on different surfaces [18], including single crystals [19] and references

\* Corresponding author. Tel.: +1 334 844 3404; fax: +1 334 844 3400.  
E-mail address: [vzp0002@auburn.edu](mailto:vzp0002@auburn.edu) (V.A. Pedrosa).

therein]. The electroreduction of  $\text{H}_2\text{SeO}_3$  is a complex process that depends on several factors such as (i) sensitivity to the electrodic surface; (ii) underpotential deposition; (iii) semiconductor compound formation; and (iv) coupled chemical reactions. The most efficient electrochemical way to produce crystalline and amorphous films of selenium is by cathodic reduction of selenious ions in an acid medium [19]. Some authors previously postulated that the electrodeposition of Se occurs following Reaction (1) [21]:



This reaction was studied by Santos and Machado [21] using the EQCM-Pt electrode in acid media, which showed that the anodic responses of mass variations were divided in three well-defined potential regions. It showed that the third region between 1.1 and 1.5 V could be attributed to the  $\text{Se} + \text{H}_2\text{O}$  dissolution peak and the Pt oxide formation. However, Solaliendres et al. [22] have reported that the selenium underpotential processes involved the formation of  $\text{H}_2\text{Se}$  species onto Au electrode in perchloric acid solution. An EQCM combined with voltammetric techniques was employed to elucidate the  $\text{H}_2\text{Se}$  reduction mechanism. Some authors suggested that at more negative potentials, specifically, the formation of the  $\text{H}_2\text{Se}$  species for the direct reduction of  $\text{Se}^{4+}$  to  $\text{Se}^{2-}$ , occur with the transference of six electrons in accordance with Reaction (2) [16,17]:



Up to now, the electrochemical behavior of selenium has not been yet fully investigated. In this way, the aim of this work is to report electrochemical results concerning the selenium deposition on quartz crystal gold electrodes from a sulphuric acidic solution. With that, the mechanisms the several processes concerning selenium electrodeposition have been investigated using several techniques, such as electrochemical quartz crystal microbalance, chronoamperometry, and cyclic voltammetry. All these results were integrated with the nanogravimetric results. In previous studies, the electrochemical behavior of selenium was investigated with emphasis in partial processes like UPD, bulk deposition or  $\text{H}_2\text{Se}$  formation or exploring aspects related to the adsorption of anions and hydrogen reduction reaction as a stage of intermediates formation [5,7,16–22].

In this way, the objective of this work is to perform simultaneous voltammetric and nanogravimetric measurements in order to obtain the respective mass/charge relationships. In an extensive potential window, this study can bring more details in the electrodeposition of Se on polycrystalline Au surfaces, from an acidic electrolyte. It will be proposed an electrochemical model for such complex electrode reaction.

## 2. Experimental

### 2.1. Chemicals

$\text{SeO}_2$  (99.99% purity) and sulphuric acid (Suprapur) were obtained from Merck and used as received. Millipore-Q purified water was used to prepare all solutions, which, previously to the experiments, were deaerated with high-purity  $\text{N}_2$  (White Martins SS) and the experiments were carried out at room temperature.

### 2.2. Equipments and apparatus

The electrochemical instrumentation consisted of an Autolab potentiostat (PGSTAT30, Ecochimie, The Netherlands) linked to a PC-AMD K6-II microcomputer and to a quartz crystal microbalance

RQCM Maxtek Inc<sup>®</sup>. The appropriate softwares were employed from AUTOLAB and Maxtek Inc<sup>®</sup>, respectively.

The working electrode (Au-EQCM) was a 5 MHz AT-cut quartz crystal disc with a diameter of 12.5 mm. Both sides of the quartz crystal were covered with thin gold films on a Ti adhesion layer, but only one of these faces (a disc of 1.37 cm<sup>2</sup> geometric area) was exposed to the electrolyte. The electrochemical area was evaluated as 4.9 cm<sup>2</sup> based on measurements of the voltammetric charge related to the reduction of a complete monolayer of gold oxide, following the Trasatti and Petrii procedure [23,24]. This procedure gives a roughness factor (*R*) value of 3.6 for the Au-EQCM electrode. All charge densities or surface coverage referred to in this work is related with such electrochemical area. The reference electrode was an Ag/AgCl (3 M KCl) and the auxiliary electrode was a Pt foil with geometric area of 1 cm<sup>2</sup>.

### 2.3. Preparation of Se thin films

The Se thin films were deposited onto Au-EQCM by potentiostatic polarization (+0.10 V) at different times ( $t = 30, 60, 120, 300, 400$  and 600 s) in 1.0 M  $\text{H}_2\text{SO}_4$  + 1 mM  $\text{SeO}_2$  ( $E_{\text{eq.}} = +0.70$  V;  $t = 2$  s), without magnetic stirring.

### 2.4. Atomic Force Microscopy

The AFM experiments were carried out with an Explorer model from Digital Instruments<sup>®</sup> model Multimode. To minimize the surface deformation and material removal, the experiments were performed in intermittent non-contact mode, using a silicon cantilever with a spring constant of 70 N m<sup>-1</sup> at a scan rate of 1 Hz. All measurements were taken under air at room temperature, employing the root mean square roughness ( $R_{\text{rms}}$ ) to compare the surfaces quantitatively and evaluate the topological changes on the plates. As the roughness value depends on the observation scale, all experiments were carried out on a scale of 1 μm. After selenium deposition, all electrodes were rinsed with Millipore water before AFM imaging. We ensured that the electrodes were perfectly clean before each experiment by successive cleaving, rising with Millipore water, and imaging in air.

## 3. Results and discussion

### 3.1. Voltammetric responses during the selenium deposition process

The voltammetric behavior for the Au-EQCM electrode immersed in 1.0 M  $\text{H}_2\text{SO}_4$  and 1.0 mM  $\text{SeO}_2$  electrolyte is shown in Fig. 1. The electrode potential was swept between 1.60 V (initial and final potential) and -0.55 V (inverse potential) at 0.10 V s<sup>-1</sup>. The dotted line showed the steady-state voltammetric profile for Au-EQCM in the absence of  $\text{SeO}_2$  (Fig. 1). Based on previous reports [22], the assignment of these voltammetric peaks ( $R_1, R_2, R_3, R_4$ ) is as follows: reduction of the Au oxide ( $R_1$ ), underpotential deposition of Se ad-atoms ( $R_2$ ), deposition of bulk selenium ( $R_3$ ), and formation of  $\text{H}_2\text{Se}$  ( $R_4$ ) in a direct reduction by 6 electrons of  $\text{Se}^{4+}$ . In the reverse scan, the observed peaks are usually attributed to the bulk Se oxidation ( $\text{Ox}_1$ ), the Se ad-atoms oxidation ( $\text{Ox}_2$ ), and the Au surface, or Au–Se alloy as described by several authors, oxidation ( $\text{Ox}_3$ ) [17–22,25–27]. All these peaks are the main subject of the present paper and will be explored in the following section.

### 3.2. Se UPD process

Although the UPD Se had already been studied, it certainly is an extremely interesting electrochemical process and deserves addi-

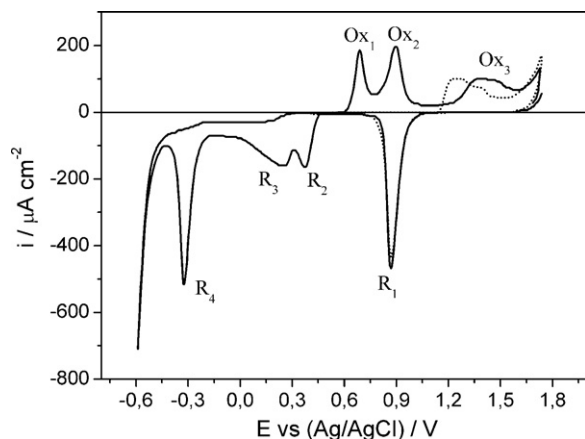


**Fig. 1.** Cyclic voltammogram for the Au-EQCM electrode in 1.0 mM  $\text{SeO}_2$  + 1.0 M  $\text{H}_2\text{SO}_4$ . The dotted line represents the response in 1.0 mol  $\text{L}^{-1}$   $\text{H}_2\text{SO}_4$ . Scan rate = 0.10  $\text{V s}^{-1}$ .

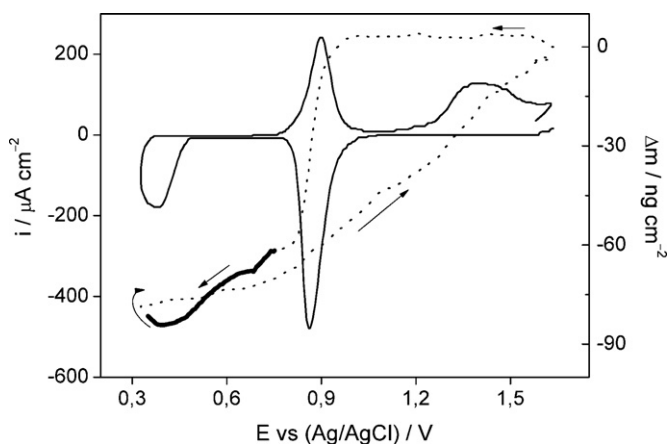


**Fig. 2.** Voltammetric profile for the Se UPD process. Cyclic voltammogram (full line) and massogram (dotted line) profiles for the Se atomic layer obtained in 1.0 mM  $\text{SeO}_2$  + 1.0 M  $\text{H}_2\text{SO}_4$ . Scan rate = 0.10  $\text{V s}^{-1}$ .

tional investigations [21,22]. We performed experiments in which the initial potential was set to 1.60 V and swept in the negative direction, showing that the UPD Se starts at about 0.35 V, while the respective re-oxidation of the monolayer occurs at approximately 0.70 V. The charge density for  $\text{Se}_{\text{ads}}$  oxidation obtained from the voltammetric profile, presented in Fig. 2, was 162  $\mu\text{C cm}^{-2}$ . This value corresponds to the charge required for the formation of 0.4 monolayer of Se ad-atoms on the Au surface, considering that a complete oxygen monolayer on gold ( $\text{AuO}^1$ ), where each  $\text{O}_{\text{ads}}$  atom occupies one Au surface atom, involves 390  $\mu\text{C cm}^{-2}$  [23,24,26–28]. In this way, taking into account that each Se ad-atom occupies two Au surface atoms with the transference of 4 electrons per ad-atom, the amount of  $\text{Se}_{\text{ads}}$  on Au surface is correspondent to 0.4 monolayer [29]. To confirm such results, we carried out EQCM experiments to determine the mass variation associated to the monolayer formation in the potential window between 0.75 and 0.35 V. The results can be seen as the massogram (highlighted line) in Fig. 2.

The theoretical mass variation associated with the formation of a complete  $\text{Se}_{\text{ads}}$  monolayer can be calculated assuming that, on polycrystalline Au surface, there are available, as adsorbing sites,  $2.16 \times 10^{-9}$  mol of Au atoms per square centimeter [30,31]. In this

way, using the molar mass of Se as 78.96  $\text{g mol}^{-1}$ , it is possible to find a theoretical value of 87.0  $\text{ng cm}^{-2}$ , considering that each  $\text{Se}_{\text{ads}}$  occupies two Au sites. This value is then associated to the reduction of  $\text{Se}^{4+}$  from the solution and the formation of a full monolayer of  $\text{Se}_{\text{ads}}$  on the Au surface. The experimental value obtained from Fig. 2 was 36.0  $\text{ng cm}^{-2}$ , which is in agreement with the charge density from the voltammetric experiments of Fig. 1 for 0.4 monolayer of Se ad-atoms. Such coverage values for Se ad-atoms on Au surface have already been reported by Furuya and Motoo [28]. However, in our work, the experimental value is not obtained as a loss of mass, but instead as an expected gain of mass. Thus, the simple scheme  $\text{Se}^{4+} + 4\text{e}^- \rightarrow \text{Se}_{\text{ads}}$  does not justify the experimental behavior.

Consequently, some interesting aspects in the massogram curve remain unclear and justify a deeper analysis. In this way, the next step is to develop an empirical model that allows us to quantitatively analyze the massogram showed in Fig. 2. From previously published work, it has been established that at 1.6 V, the initial potential of the massogram, the electrode surface is fully oxidized and covered with a sub-monolayer of adsorbed  $\text{H}_2\text{SeO}_3$  molecules, which was originated from the dissolution of  $\text{SeO}_2$  in the acid electrolyte [32].

Controversy can be found in the literature concerning the adsorption of  $\text{H}_2\text{SeO}_3$  on gold surfaces. Some authors previously concluded that such species do not seem to adsorb on Au or AuO surfaces [33]. In order to clarify such possibility, we performed an adsorption experiment, in which the quartz crystal microbalance gold electrode was polarized at 1.60 V until stabilization of the mass profile and then 1 mM  $\text{SeO}_2$  was added to the electrolyte (1.0 M  $\text{H}_2\text{SO}_4$ ). A total of 120.0  $\text{ng cm}^{-2}$  positive mass variation was obtained up to mass profile stabilization, as presented in Fig. 3. This mass value corresponds to 0.85 monolayers of  $\text{H}_2\text{SeO}_3$  adsorbed on AuO surfaces (each molecule occupying two surface sites). In this way, our experiment showed, without doubt, that  $\text{H}_2\text{SeO}_3$  does adsorb on the AuO surface, which justifies the discussions below.

Scanning towards the negative direction, no mass change is detected until the potential values reach approximately 1.0 V, where AuO begins to be reduced. Such transformation should promote a loss of mass of approximately 35.0  $\text{ng cm}^{-2}$  (same considerations as above for  $\text{Se}_{\text{ads}}$ , but using the molar mass of oxygen, 16.0  $\text{g mol}^{-1}$ ). In the experimental result showed in Fig. 2, a loss of mass of 75.0  $\text{ng cm}^{-2}$  can be detected in the potential range between 1.0 and 0.80 V, much larger than the expected one. This behavior is not observed in the blank solution (with only  $\text{H}_2\text{SO}_4$  in the electrolyte), thus suggesting that it cannot be associated to  $\text{HSO}_4^-$  adsorption. Clearly, the excess of mass should be attributed

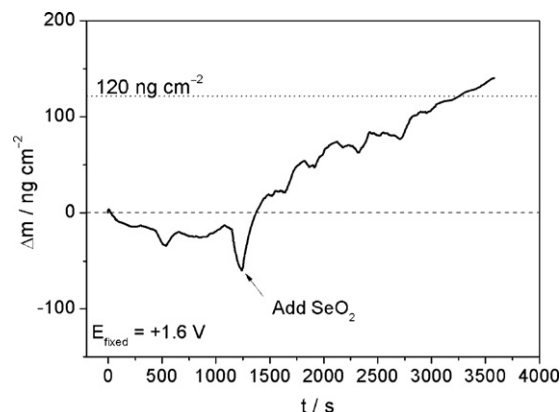
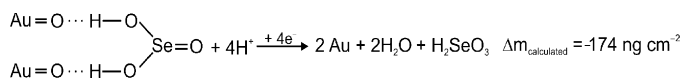
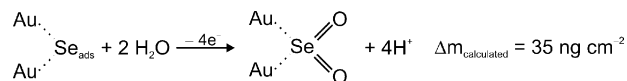


**Fig. 3.** Mass-time gravimetric curve obtained with the Au-EQCM electrode before and after the addition of an aliquot of  $\text{SeO}_2$  in 1.0 M  $\text{H}_2\text{SO}_4$ . Final concentration of  $\text{SeO}_2$  equals to 1 mM. Electrode potential fixed at +1.60 V.

<sup>1</sup> AuO does not correspond to the phase oxide layer. AuO indicated a full monolayer of oxygen ad-atoms on gold surface.



Scheme 1.



Scheme 3.

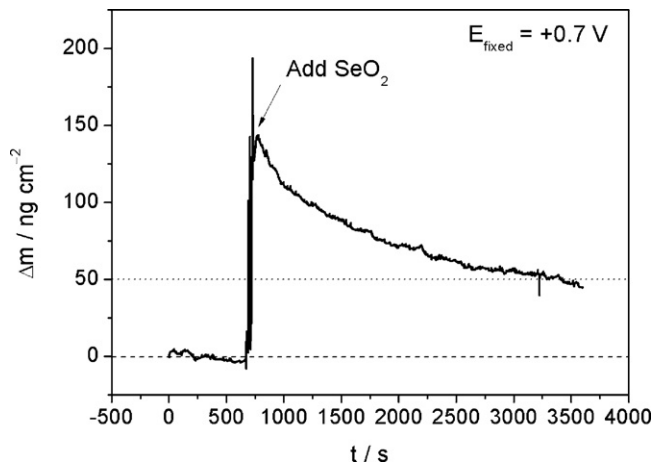


**Fig. 4.** Mass-time gravimetric plots obtained with the Au-EQCM electrode before and after the addition of  $\text{SeO}_2$  to the 1.0 M  $\text{H}_2\text{SO}_4$  electrolyte. Final concentration of  $\text{SeO}_2$  equals to 1 mM. Electrode polarized at +0.70 V.

to a sub-monolayer of  $\text{H}_2\text{SeO}_3$  adsorbed that leaves the electrode surface together with the oxygen ad-atoms during the AuO reduction as follows:

The amount of mass left to the  $\text{H}_2\text{SeO}_3$  desorption is around  $40.0 \text{ ng cm}^{-2}$ , much less than expected for a full coverage (Scheme 1). Most likely included in this balance is the re-adsorption of a fraction of selenic acid on the Au newly reduced surface, after some kind of rearrangement. This adsorbed selenic acid species should provide the 0.4 monolayer of  $\text{Se}_{\text{ads}}$ , as found in the voltammetric experiments, which will be justified in the next paragraph. To complete the balance, the initial coverage with  $\text{H}_2\text{SeO}_3$  should be taken as 0.7 monolayer, a little less than the maximum coverage showed in Fig. 3 (0.85 monolayer). However, we have to consider that the adsorption time on polarized electrode should be less than the 20 min took to obtain the maximum coverage in Fig. 3.

Aiming to investigate the possible adsorption of  $\text{H}_2\text{SeO}_3$  on reduced gold surfaces, we performed the quartz crystal microbalance experiment and reported the results in Fig. 4. Here the Au electrode was kept polarized at 0.70 V during 750 s for the mass stabilization, followed by the addition of 1 mM  $\text{SeO}_2$  to the electrolyte (again, 1.0 M  $\text{H}_2\text{SO}_4$ ). The initial rising of approximately  $150.0 \text{ ng cm}^{-2}$  can be justified by the adsorption of several disordered monolayers of  $\text{H}_2\text{SeO}_3$  on the surface. After that, the electrode coverage begins to organize until, finally, only a sub-monolayer of adsorbed selenic acid remains on the surface. The total mass variation, between the  $\text{SeO}_2$  addition and this stabilized film formation – around 50 min of immersion – is about  $50.0 \text{ ng cm}^{-2}$ , or approximately 0.4 monolayer of  $\text{H}_2\text{SeO}_4$ . So, it is also possible to postulate that the selenic acid can adsorb on reduced Au surface generating coverages as high as 0.4 monolayers.

The next electrode process that occurs on this newly reduced surface is the formation of the Se ad-atoms monolayer, originated from the 0.4 monolayer of adsorbed  $\text{H}_2\text{SeO}_3$ , which begins at 0.75 V. Here the general scheme should be:



Scheme 2.

The theoretical mass variation shown in Scheme 2 corresponds to the transformation of 0.4 monolayer of selenic acid adsorbed in the Au surface (as discussed before) in  $\text{Se}_{\text{ads}}$ . The experimental value obtained ( $23.0 \text{ ng cm}^{-2}$ ), highlighted in the massogram of Fig. 2, is in full agreement with the proposition of only 0.4 monolayer of  $\text{Se}_{\text{ads}}$  and is formed, thus confirming the voltammetric charge measurement.

At 0.35 V, in the end of  $\text{Se}_{\text{ads}}$  process, the potential sweep is switched to the positive direction. Up to +0.80 V was observed as only a slightly rising in mass ( $12.0 \text{ ng cm}^{-2}$ ) and can probably be associated to water (or anions) adsorption on top of the  $\text{Se}_{\text{ads}}$  layer. At 0.80 V, the voltammogram in Fig. 2 showed the beginning of  $\text{Se}_{\text{ads}}$  oxidation, with a well-defined voltammetric peak at 0.89 V. This process is normally associated with a loss of mass of approximately  $87.0 \text{ ng cm}^{-2}$ . However, in Fig. 2 it is possible to observe, in this potential region, a mass gain of approximately  $40.0 \text{ ng cm}^{-2}$  associated to an anodic voltammetric charge of  $162 \mu\text{C cm}^{-2}$ . This unexpected behavior should be associated to Scheme 3.

Thus, the voltammetric oxidation peak does not promote the redissolution of adsorbed Se except its oxidation, followed by oxygen incorporation. This causes the rise in the mass by a value similar to the value obtained through calculation.

The adsorbed  $\text{SeO}_2$  blocks the electrode surface and inhibits the formation of AuO. In this way, in the voltammetric response, the onset of surface oxide formation is shifted to potentials more positive than 1.20 V, while in the massogram there is a plateau, meaning that no change in the electrode mass is occurring. After 1.20 V, the Au surface begins to oxidize, resulting in the gain of mass of approximately  $50.0 \text{ ng cm}^{-2}$  following the scheme below:

One important aspect of this general scheme is that the cycle closes and the electrode returns to the same mass it presented in the beginning of the potential scan.

To perform a deeper investigation on the nature of the UPD  $\text{Se}_{\text{ads}}$  oxidation peak at 0.90 V, we performed the experiment presented in Fig. 5, which shows the  $\Delta m/\Delta q$  plot. This relationship is a representation of Faraday's law, obtained by calculating the charge variation from the voltammogram and the mass variation from the massogram for each potential step. The slope of each linear segment of such plot is related with the molar mass of the electroactive species. An analysis of Fig. 5 shows a straight line obtained between 0.80 and 0.95 V, followed by an exponential section up to 1.0 V. This last section can be roughly approximated by a "linear" fitting. The

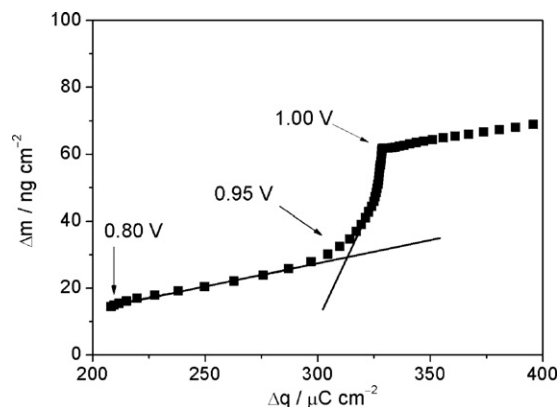
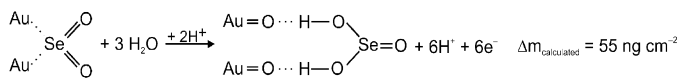


**Fig. 5.**  $\Delta m$  vs  $\Delta q$  plots for Se UPD oxidation. The slope value for the linear region is included.



Scheme 4.

slope of the first section is calculated as  $1.5 \times 10^{-4} \text{ g C}^{-1}$ .

$$\Delta Q = nF\Delta N = \frac{nF\Delta m}{M} \quad (3)$$

$$M = \frac{nF\Delta m}{\Delta Q} = nF \text{ slope} \quad (4)$$

Using the Faraday equation, a value of molar mass ( $M$ ) of  $14.5 \text{ g mol}^{-1}$  is obtained, considering the number of electrons ( $n$ ) equals one. This corresponds to the reaction involving oxygen atoms adsorbed on two sites of the Au surface. This fits quite well in the scheme shown in Eqs. (5) and (6). The last section in Fig. 5, from 0.95 to 1.0 V, corresponds to a deep increase in mass without some considerable variation in charge. This process yielded an exponential dependence that can be attributed the adsorption of water and anions on the  $\text{Au}_2\text{Se}(\text{OH})_2$  surface as an approximation of the processes depicted in Scheme 4.

### 3.3. Se bulk process

The first cyclic voltammetric response for bulk Se deposition is presented in the highlighted region of Fig. 6, showing that Se bulk deposition starts immediately after the underpotential deposition region, as previously reported on polycrystalline gold [22]. Furthermore, the integrated area under peak  $\text{O}_1$  (associated with the bulk Se redissolution) was calculated to be approximately  $374 \mu\text{C cm}^{-2}$ . Such bulk deposition must occur on top of the previously formed UPD monolayer, whose charge was found to be  $162 \mu\text{C cm}^{-2}$  in the previous section. If a few bulk layers follow a certain epitaxial behavior, the charge previously determined for bulk Se should correspond to approximately 2.3 layers. Of course, in this case, the deposition/dissolution potentials shifted to the Nernstian value, since no more Se–Au interactions were in course.

The mass variations that occurred during the potential scanning are also presented in Fig. 6 as the dot line. In the bulk deposition region (between 0.35 and 0.0 V in the negative potential scanning and 0.0–0.2 V in the positive direction, after the potential sweep inversion at 0.0 V), a sharp increase in mass is observed, whose value is approximately  $120.0 \text{ ng cm}^{-2}$ . If, as in the previous sec-

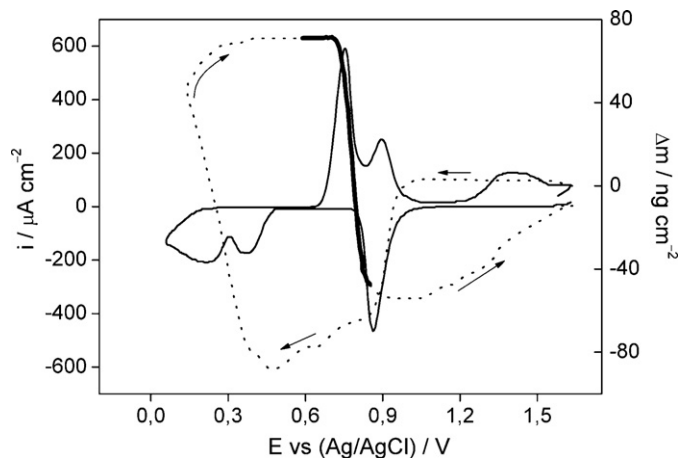


Fig. 6. Voltammetric behavior of Se bulk process. Cyclic voltammogram (full line) and massogram (dotted line) profiles for Se in  $1.0 \text{ mM SeO}_2 + 1.0 \text{ M H}_2\text{SO}_4$ . Scan rate =  $0.10 \text{ V s}^{-1}$ .

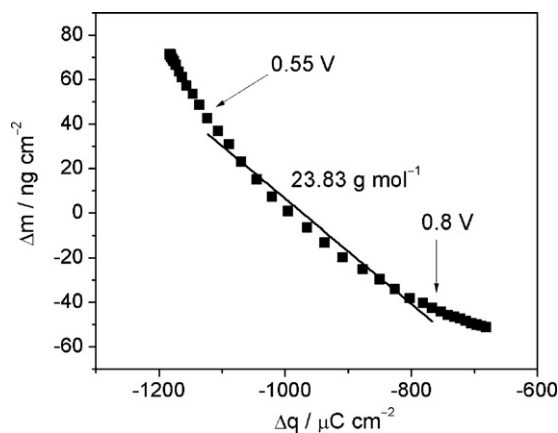


Fig. 7.  $\Delta m$  vs  $\Delta q$  plots for selenium bulk oxidation. The slope values for the linear region is included.

tion, we consider the mass increase for each  $\text{Se}_{\text{ads}}$  complete layer as  $(0.4 \times 85) \text{ ng cm}^{-2}$ , the  $\Delta m$  value found for bulk deposition corresponds to approximately 3.5 layers, which must be handled with care due to the lack of epitaxy with the growing of some layers. So, this value is satisfactory with the voltammetric one (2.3 layers observed).

For bulk Se dissolution, the mass profile shows a large decrease towards more positive potential, as the amount of Se decreases, from Fig. 6. The observed loss of mass is about  $100.0 \text{ ng cm}^{-2}$ , meaning that, at least  $20.0 \text{ ng cm}^{-2}$  of  $\text{Se}_{\text{ads}}$  remain in the electrode surface, possibly due to a closest package of the first monolayer. It must be emphasized that similar results have already been obtained for the bulk electrochemical behavior of Se on polycrystalline gold [23,32–35].

In Fig. 7, the nature of this electrochemical process is further analyzed based in the  $\Delta m/\Delta q$  plot related with the potential region for bulk Se oxidation (0.53–0.80 V in Fig. 6). As before, the slope of the straight line obtained is related with the molar mass of the reagent the Faraday's law (Eqs. (3) and (4)). Here, we found a value of  $2.47 \times 10^{-4} \text{ g C}^{-1}$  for the bulk Se oxidation. By multiplying by the Faraday constant, i.e.,  $96,487 \text{ C mol}^{-1}$  and by the number of electrons transferred in the process (4) a molar mass value of  $95.0 \text{ g mol}^{-1}$  can be obtained, which is close to the theoretical value for  $\text{Se}^{4+}$  ( $79.0 \text{ g mol}^{-1}$ ). As the electrodeposition of bulk Se proceeds through a very complex multi-step process, the  $\Delta m/\Delta q$  slope value obtained can be considered in good agreement with the atomic mass for Se.

### 3.4. Electrochemical formation of $\text{H}_2\text{Se}$

Further expanding the negative potential window of the Au/Se electrode up to  $-0.50 \text{ V}$  gives rise to a new cathodic process described by some authors as the direct reduction of  $\text{Se}^{4+}$  to  $\text{Se}^{2-}$  (in a six electron process) and by others as the initial reduction of  $\text{Se}^{4+}$  to Se followed by Se to  $\text{Se}^{2-}$  in two half-reactions [5,16,22,36]. At room temperature,  $\text{H}_2\text{Se}$  is a gas. Thus, it nucleates, grows forming bubbles, and detaches from the electrode surface. Such gas evolution consumes the bulk Se phase, and consequently, the bulk Se redissolution should generate a smaller electrochemical (or nanogravimetric) response.

In this work, we have studied the  $\text{H}_2\text{Se}$  formation process as the last segment of the electrode potential sweep towards negative direction. Here, the  $\text{H}_2\text{Se}$  is generated as the reduced product of few monolayers of bulk Se deposited during the scanning, i.e., approximately three monolayers.

In the potential range related to the  $\text{H}_2\text{Se}$  nanogravimetric response, shown highlighted in Fig. 8, we observed a loss of mass

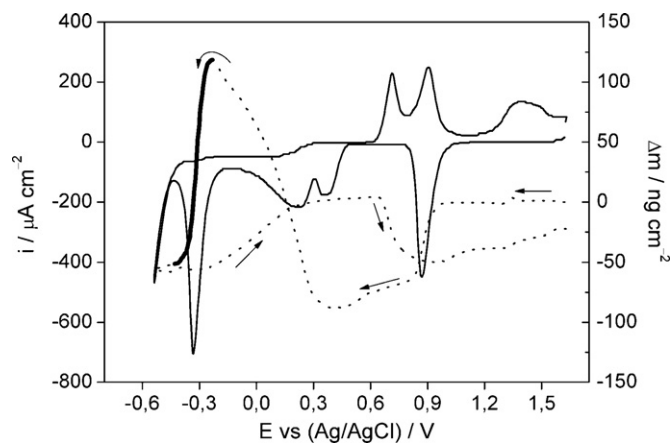
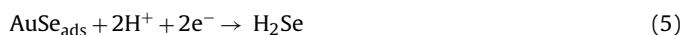


Fig. 8. Cyclic voltammogram and massogram profiles for selenium electrochemical processes on Au-EQCM in 1.0 mM  $\text{SeO}_2 + 1.0 \text{ M H}_2\text{SO}_4$ . Scan rate =  $0.10 \text{ V s}^{-1}$ .

of approximately  $170.0 \text{ ng cm}^{-2}$ , which suggests that bulk Se is leaving the electrochemical surface. This mass variation value is higher than that discussed in the previous section for bulk Se, because, as the potential scanning is now conducted up to more negative values, the amount of bulk Se obtained on the electrode surface is also higher than in the previous case. Scanning between 0.40 and  $-0.25 \text{ V}$  allows the deposition of approximately  $200.0 \text{ ng cm}^{-2}$  of bulk Se. After  $-0.25 \text{ V}$ , the reduction of such bulk Se occurs, generating  $\text{H}_2\text{Se}$  and causing the Se dissolution, as in the scheme below:



There is some controversy in literature about the extension of the contribution from Reactions (3) or (4) for the cathodic peak in the voltammogram shown in Fig. 8 [5,16,22,36].

These electroreduction processes are associated with a voltammetric cathodic peak at  $-0.35 \text{ V}$  and a charge value of  $600 \mu\text{C cm}^{-2}$ . As before, considering that a full monolayer of  $\text{H}_2\text{Se}$  would involve a charge density of  $185 \mu\text{C cm}^{-2}$  (two electrons transferred and two active sites occupied by each  $\text{H}_2\text{Se}$  molecule) and a loss of mass somewhat higher than  $(0.4 \times 87.5) \text{ ng cm}^{-2}$ , the values reported above suggest a loss of approximately three monolayers of  $\text{Se}_{\text{ads}}$ , due to its electroreduction to  $\text{H}_2\text{Se}$ . Finally, the hydrogen evolution reaction promotes the cathodic currents observed around  $-0.55 \text{ V}$ .

In the reverse scan, after the hydrogen evolution reaction, at potentials more positive than  $-0.40 \text{ V}$ , the cathodic current observed in Fig. 8 shows diffusion controlled behavior due to the bulk Se deposition until the electrode potential reaches approximately  $0.30 \text{ V}$ . The mass variation associated to such deposition was found to be approximately  $60.0 \text{ ng cm}^{-2}$ , and the amount of Se deposited should be added to the remaining  $\text{Se}_{\text{ads}}$  after the potential incursion towards the  $\text{H}_2\text{Se}$  formation region, to generate the Se bulk phase that will be oxidized at  $0.70 \text{ V}$ . At this potential value, the anodic peak observed is due to the dissolution of Se bulk and has a loss of mass of  $55.0 \text{ ng cm}^{-2}$  associated with it. This is a mass value lower than that expected by the amount of  $\text{Se}_{\text{ads}}$  in the bulk phase, which can be associated to some intermetallic Au–Se compound, stable at this potential window, as already reported [16,25]. As previously observed, the oxidation of the UPD Se, at  $0.90 \text{ V}$ , promotes a gain of mass indicating that  $\text{Se}^{4+}$  does not leave the electrode surface, but instead forms the corresponding oxygenated species ( $\text{SeO}_3^{2+}$ ).

Finally, the mass variation observed in Au oxidation potential region was approximately  $25.0 \text{ ng cm}^{-2}$  as showed in Fig. 8. This value is very close to that calculated for the adsorption of a complete monolayer of oxygen onto gold electrode (i.e.,  $32.0 \text{ ng cm}^{-2}$

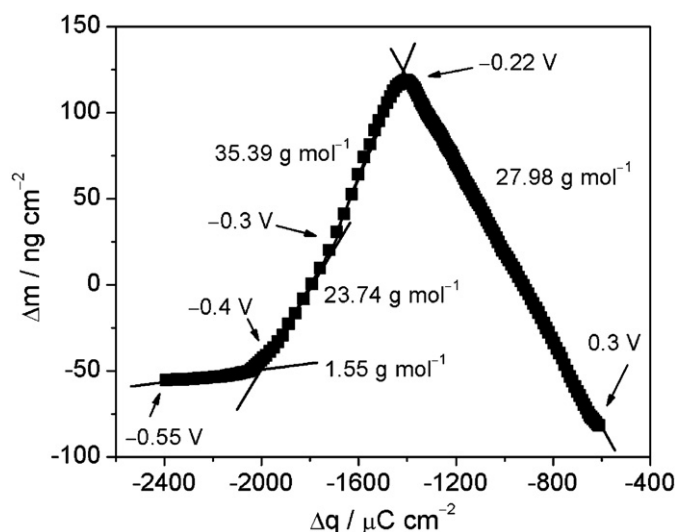


Fig. 9.  $\Delta m$  vs  $\Delta q$  plots for selenium bulk reduction and  $\text{H}_2\text{Se}$  formation showed in Fig. 8. The slope values for the linear region are included.

as discussed in the item before). This lower value can also be a consequence of the formation of the Au–Se surface alloy.

### 3.5. Mass variations to electrochemical processes involving $4\text{e}^-$ or $6\text{e}^-$

The  $m/z$  analysis of the electrochemical process during the electroreduction of  $\text{Se}^{4+}$  in the  $\text{H}_2\text{Se}$  potential region is shown in Fig. 9. In accordance with Kazacos and Miller, a study of the reduction of selenious acid and in  $\text{H}_2\text{SO}_4$  solution has shown that the initial cathodic reaction involves an overall transfer of six electrons [16,17]. Two molecules of the newly formed  $\text{H}_2\text{Se}$  may react in the presence of  $\text{H}_2\text{SeO}_3$  from the bulk solution, yielding elemental selenium. The rate of the chemical reaction is dependent on the concentration of  $\text{H}_2\text{SeO}_3$  and is sufficiently rapid at high  $\text{H}_2\text{SeO}_3$  concentrations.

The analysis of  $m/z$  relationship has been performed in the potential range between  $0.32$  and  $-0.6 \text{ V}$  as detailed in Fig. 9 (experimental data obtained from the voltammogram and the massogram presented in Fig. 8). We consider a table involving three electrochemical reactions (Table 1).

Initially, the electrodeposition process started with the transference of four electrons, in the potential region between  $0.32$  and  $-0.22 \text{ V}$  (bulk Se deposition). The theoretical  $m/z$  relationship for this reaction is  $33.2 \text{ g mol}^{-1}$  thus, experimental data,  $28.0 \text{ g mol}^{-1}$ , presents an excellent agreement. In the next potential range ( $-0.2$  to  $-0.31 \text{ V}$ ), in the beginning of  $\text{H}_2\text{Se}$  formation, it is observed that the reduction of  $\text{Se}^0$  to  $\text{Se}^{2-}$  predominates with a transference of two electrons, which seems to be confirmed by the experimental and theoretical  $m/z$  values (experimental  $m/z$  value was  $-35.4 \text{ g mol}^{-1}$  and the theoretical one is  $-40.5 \text{ g mol}^{-1}$ ). Finally, in the potential region between  $-0.31$  and  $-0.40 \text{ V}$ , another very good agreement between theoretical and experimental  $m/z$  relationships ( $-22.5 \text{ g mol}^{-1}$  and  $-23.7 \text{ g mol}^{-1}$  respectively) points to a transference of six electrons, probably as a consequence of

Table 1  
Reactions and  $m/z$  theoretical values of selenium in aqueous solution.

Reactions	$m/z_{\text{theoretical}}$
$\text{H}_2\text{SeO}_3 + 4\text{H}^+ + 4\text{e}^- \rightarrow \text{Se}^0 + 3\text{H}_2\text{O}$	$33.24 \text{ g mol}^{-1}$
$\text{Se}^0 + 2\text{H}^+ + 2\text{e}^- \rightarrow \text{H}_2\text{Se}$	$-40.48 \text{ g mol}^{-1}$
$\text{H}_2\text{SeO}_3 + 6\text{H}^+ + 6\text{e}^- \rightarrow \text{H}_2\text{Se} + 3\text{H}_2\text{O}$	$-22.49 \text{ g mol}^{-1}$

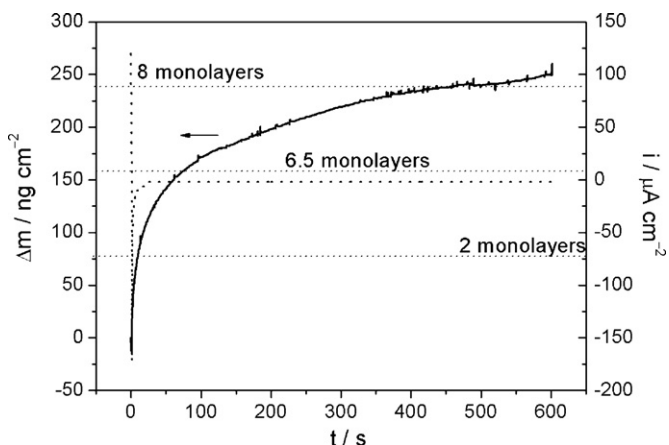


**Fig. 10.** Gravimetric and potentiostatic current transient for the electrodeposition of  $\text{H}_2\text{SeO}_3$  on Au electrode at  $+0.10\text{ V}$ . The dotted line corresponds to the stationary current for Se deposition, while the full line represents the corresponding mass variation during the deposition time. The grid lines are included to illustrate the theoretical mass variation values corresponding to the formation of 2, 6.5 and 8 monolayers of deposited bulk Se.

the high overpotential applied in the electrode. At more negative potentials, only the HER ( $m/z$  theoretical =  $-2.0\text{ g mol}^{-1}$  and experimental =  $-1.5\text{ g mol}^{-1}$ ) can be found.

### 3.6. Characterization of selenium thin films

In the preparation of thin films, it is important to control film properties such as homogeneity and porosity in order to obtain high-quality coverages. Electrochemistry has been proven to be a very helpful tool since it provides information about several processes taking place during the film formation [37–39].

In this work, Se thin films were obtained by chronoamperometric experiments where the Au-EQCM electrode was polarized at  $+0.10\text{ V}$  during 600 s in an electrolyte composed of  $1.0\text{ M H}_2\text{SO}_4 + 1.0\text{ mM SeO}_2$ . The correspondent deposition charge was evaluated from the area under the curve, as depicted in Fig. 10. After several experiments, the average deposition charge was  $1.38\text{ mC cm}^{-2}$ . Considering that: (a) the theoretical charge for one Se monolayer on gold surface is  $162\text{ } \mu\text{C cm}^{-2}$  ( $0.41 \times 390$ , as detailed before), (b) each Se atom occupies two atoms on the gold surface, and (c) the growing of the Se monolayers occurs in an epitaxial mode, the calculated charge should be equivalent to approximately 8.5 monolayers [40,41]. It can also be observed in the massogram correspondent to the chronoamperogram (Fig. 10), that

a mass increase of  $250.0\text{ ng cm}^{-2}$  is obtained during the growth of the Se thin film, which corresponds to approximately 8.0 monolayers (considering that each Se monolayer requires  $31.69\text{ ng cm}^{-2}$ ). This result corroborated the chronoamperometric experiments and the epitaxial growth up to this film thickness. The film stops to grow significantly after around 400 s of deposition. This effect has been related to the fact that Se has low  $p$ -type conductivity and cuts off the cathodic current [39].

The cyclic voltammogram of an Au-EQCM electrode coated with the selenium thin film deposited, as discussed above in  $1.0\text{ M H}_2\text{SO}_4$  at  $0.10\text{ V s}^{-1}$  in the  $\text{H}_2\text{Se}$  formation region, is shown in Fig. 11A. The voltammetric profile for this film was presented in previous work, in similar experimental conditions [42]. Here, the voltammetric profile showed marked differences in relation with that discussed in the previous section, with  $\text{SeO}_2$  in the electrolyte. During a negative scan between 0.50 and  $-0.60\text{ V}$ , the reduction peak related to the  $\text{H}_2\text{Se}$  formation is observed, as well as its equivalent anodic peak in the reverse scan. This couple of peaks is attributed to the reduction of Se to  $\text{Se}^{2-}$  in the negative scan, as discussed above, and the reaction with  $\text{H}^+$  generating gaseous  $\text{H}_2\text{Se}$  species, which diffuses away from the electrochemical surface. The oxidation of  $\text{H}_2\text{Se}$  to Se promotes the anodic peak at approximately  $-0.18\text{ V}$  in the positive scan.

The mass decrease observed during the  $\text{H}_2\text{Se}$  formation, in the negative scan, shown in Fig. 11A, was  $-124.54\text{ ng cm}^{-2}$  sufficient to propose the dissolution of four monolayers of Se from the surface ( $31.69\text{ ng cm}^{-2}$  per layer, as before). In the reverse scan, during the potential range of  $-0.60$  to  $0.50\text{ V}$ , we observed a positive mass variation of  $+66.6\text{ ng cm}^{-2}$  (2.1 monolayers), which corresponds then to the re-oxidation of  $\text{H}_2\text{Se}$  to  $\text{Se}^0$ . In Fig. 11B the potential scan for a range more positive than  $0.50\text{ V}$  is presented, in which two electrochemical processes are observed at 0.90 and  $1.0\text{ V}$ , related to the oxidation of bulk Se and Se ad-atoms oxidation. The first electrochemical process in  $0.90\text{ V}$  corresponds to about 2.7 monolayers of Se, with a loss of mass of  $-88.0\text{ ng cm}^{-2}$ , very close to the results described in the voltammetric analysis of Se thin film on the Au-EQCM surface. The oxidation process at  $1.0\text{ V}$  is related to the oxidation of  $\text{Se}_{\text{ads}}$ . Apparently, this process is not affected by the evolution of  $\text{H}_2\text{Se}$  gaseous species.

The Atomic Force Microscopy images for Se film prepared under potentiostatic conditions are collected in Fig. 12. The electrodepositions were conducted at different times, as explained above. The gold electrodes used in this experiment were obtained from commercial CD-R gold surfaces. This is a simple, reproducible, and inexpensive way for the ex situ analysis with reproducible areas, and as the CD-R surfaces are obtained by chemical vapor deposition, the surface has morphologic aspects very similar to the

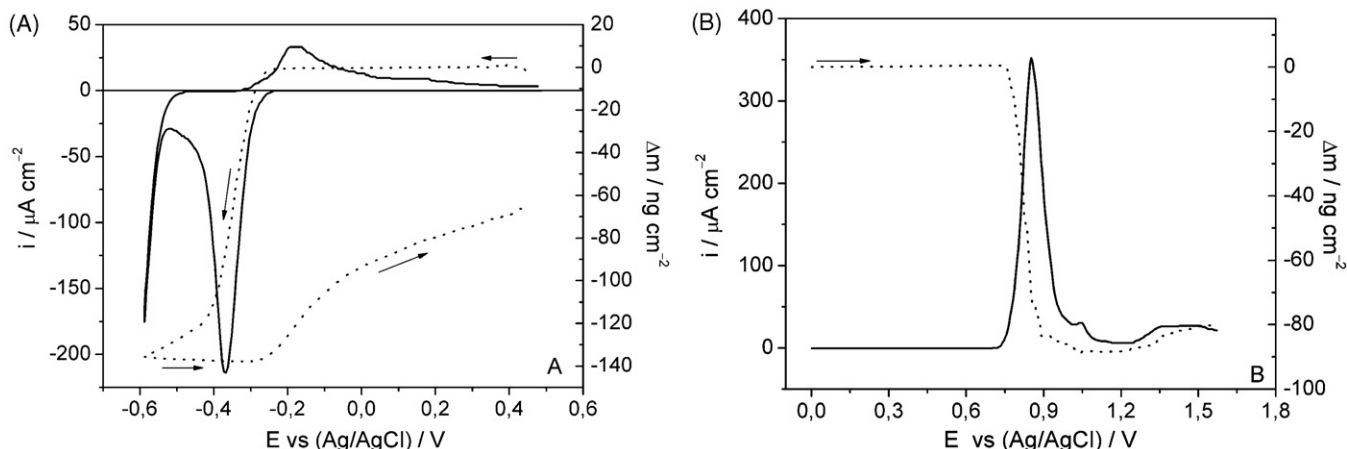


**Fig. 11.** (A) Cyclic voltammogram of the Au-film EQCM coated with Se thin film in  $1.0\text{ M H}_2\text{SO}_4$ . (B) Massogram profiles for Se thin film. Scan rate =  $0.10\text{ V s}^{-1}$ .

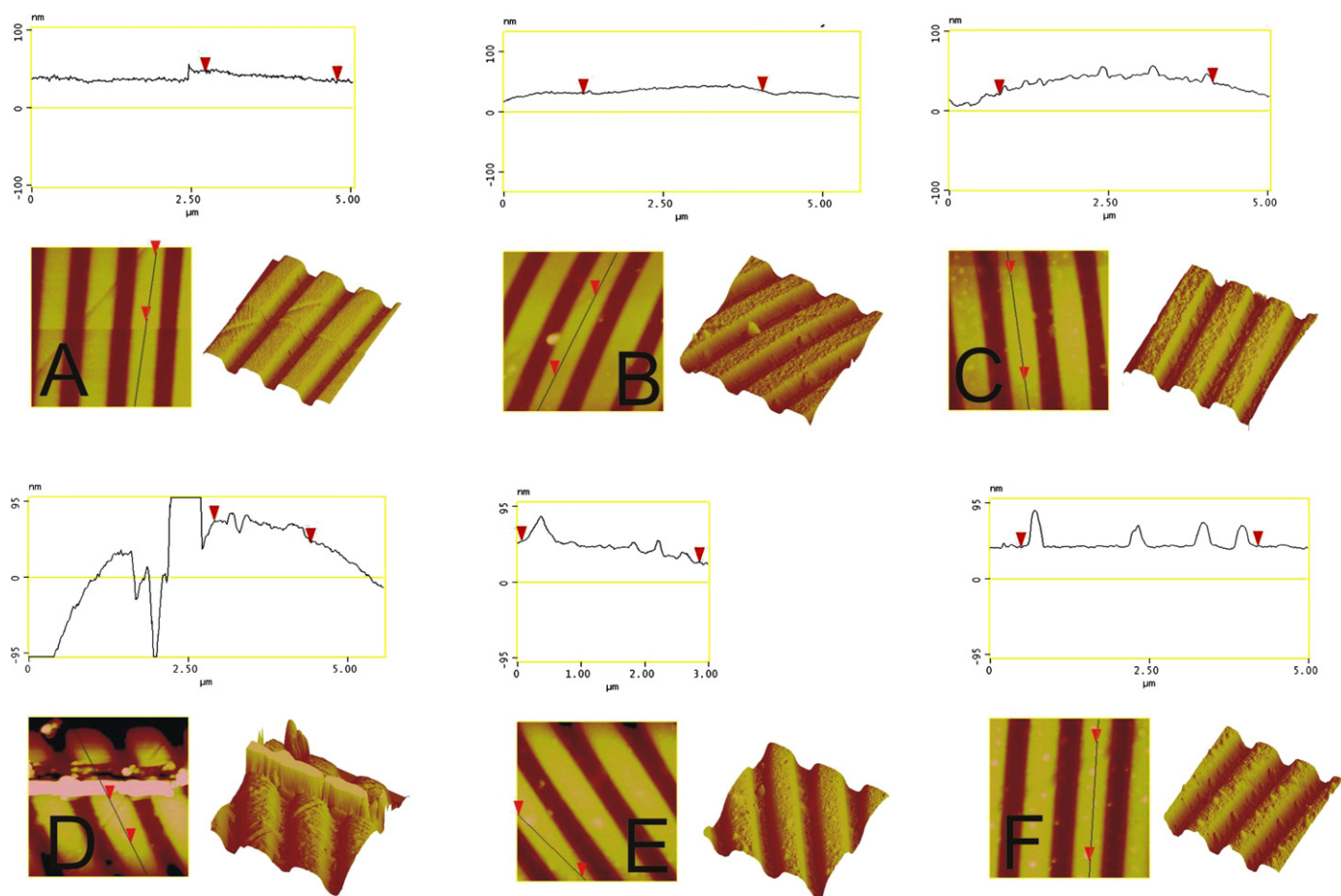


**Fig. 12.** Ex situ AFM images of CD-R gold surface, including the growth of a Au–Se thin film, in 1.0 mM  $\text{SeO}_2$  + 1.0 M  $\text{H}_2\text{SO}_4$  at different times of (A) 30 s, (B) 60 s, (C) 120 s, (D) 300 s, (E) 400 s and (F) 600 s. Electrodeposition potential = 0.10 V. Scan size =  $5 \mu\text{m} \times 5 \mu\text{m}$ .

**Table 2**

Values of roughness ( $R_{\text{rms}}$ ) of CD-R gold surface and selenium thin films.

Au-EQCM/Se coated	$R_{\text{rms}}$
Au-EQCM	3.10
Se coated ( $t = 30$ s)	3.54
Se coated ( $t = 60$ s)	4.62
Se coated ( $t = 120$ s)	6.71
Se coated ( $t = 300$ s)	7.20
Se coated ( $t = 400$ s)	8.50
Se coated ( $t = 600$ s)	13.75

EQCM electrodes [43]. AFM studies were performed to observe the topologies of the electrodeposited catalyst films. The films were deposited from different times. The Se films topology presents regular pyramidal structures (three-dimensional) and is similar to characteristics observed in the literature. The principal feature of this topology is a composition of medium islands of densely packed grains, indicating homogeneous deposition. Such morphological aspects are entirely distinct from the epitaxy observed in the previous items. However, it has to be considered that the amount of electrodeposited bulk Se here is much larger than before (about 50 monolayers or more), thus justifying the loss of epitaxy and the formation of the observed morphology. The  $R_{\text{rms}}$  values for different deposition times are presented in Table 2 and were estimated using the Nanoscope Digital Software® by the average of five different sites for the Se films samples. So, this estimative suggests the “true” roughness factor of the films and can be useful in characterization of electrochemical area in such thin films of Se.

#### 4. Conclusions

The cyclic voltammetry in simultaneous measurement with the electrochemical quartz crystal microbalance allowed an extensive discussion of every stage of Se electrodeposition on polycrystalline Au surfaces.

The analysis of charge (from the voltammograms) and mass (nanogravimetric measurements) variations have indicated a quite complex electrochemical behavior of  $\text{H}_2\text{SeO}_4$  on gold polycrystalline electrode from the first monolayer up to the deposition of thin films.

In the first stage, at positive potentials, the nanogravimetric experiments showed, beyond doubts that  $\text{H}_2\text{SeO}_3$  adsorbs on the AuO surfaces, generating a complete layer on the electrode surface. Here, we have shown for the first time, the mass variation obtained from the generation of a full monolayer of  $\text{AuO}(\text{H}_2\text{SeO}_3)$  in a simultaneous chronopotentiometric/nanogravimetric measurement. This is a very important point in this work, since its existence was an object of controversy with previously published papers. From such precursor layers, the underpotential deposition occurs followed by the bulk deposition.

Another interesting conclusion is that, in UPD conditions,  $\text{Se}_{\text{ads}}$  does not leave the electrode surface after electrooxidation reactions, but the reduction/oxidation occurs from/to  $(\text{SeO}_3^{2-})_{\text{ads}}$  instead. This means that in the reduction step, where an increase in mass value should be expected due to the formation of  $\text{Se}_{\text{ads}}$  monolayer, we instead observed a loss of mass while in the oxidation step; an increase of mass has been evidenced and not the expected loss of mass by  $\text{Se}_{\text{ads}}$  redissolution.

During the bulk Se deposition/redissolution, the electrochemical response was the expected one, and in both voltammetric and chronoamperometric depositions, we were able to show that an epitaxial (or almost) behavior occurred until the film grew to up to 8 layers. What is important to obtain is the homogeneous coverage of the surface.

Finally, the H<sub>2</sub>Se formation was studied under different conditions, and we showed that, depending on the applied potential, the reaction proceeded with the transference of four or six electrons. This was also an important point that was possible to be clarified by the nanogravimetric/voltammetric association.

### Acknowledgements

The authors thank FAPESP (proc. 04/09906-3), CNPq and CAPES for financial assistance during the execution of this work.

### References

- [1] D. Lincot, *Thin Solid Films* 487 (2005) 40.
- [2] I.M. Dharmadasa, J. Haigh, *J. Electrochem. Soc.* 153 (2006) G47.
- [3] T.S. Olson, P. Atanassov, D.A. Brevnov, *J. Phys. Chem. B* 109 (2005) 1243.
- [4] M.O. Kostin, O.H. Sheikina, *Mater. Sci.* 38 (2002) 898.
- [5] R. Vaidyanathan, S.M. Cox, U. Happek, D. Banga, M.K. Mathe, J.L. Stickney, *Langmuir* 22 (2006) 10590.
- [6] R. Vidu, N. Hirai, S. Hara, *Phys. Chem. Chem. Phys.* 3 (2001) 3320.
- [7] M.J. Esplandiu, M.A. Schneeweiss, D.M. Kolb, *Phys. Chem. Chem. Phys.* 1 (1999) 4847.
- [8] L. Xiao, L. Zhuang, Y. Liu, J. Lu, H.D. Abruña, *J. Am. Chem. Soc.* 131 (2009) 602.
- [9] M.D. Lay, J.L. Stickney, *J. Am. Chem. Soc.* 125 (2009) 1352.
- [10] L.P. Colletti, B.H. Flowers Jr., J.L. Stickney, *J. Electrochem. Soc.* 145 (1998) 1442.
- [11] M. Wanunu, A. Vaskevich, I. Rubinstein, *J. Am. Chem. Soc.* 126 (2004) 5569.
- [12] K. Shimazu, T. Kawaguchi, T. Isomura, *J. Am. Chem. Soc.* 124 (2002) 652.
- [13] X.H. Zhang, *Phys. Chem. Chem. Phys.* 10 (2008) 6842.
- [14] A. Bund, O. Schneider, V. Dehnke, *Phys. Chem. Chem. Phys.* 4 (2002) 3552.
- [15] J.O'M. Bockris, S. Fletcher, R.J. Gale, S.U.M. Khan, D.M. Kolb, D.J. Mazur, K. Uosaki, N.L. Weinberg, *Annu. Rep. Prog. Chem., Sect. C: Phys. Chem.* 92 (1995) 23.
- [16] M.Z. Kazacos, B. Miller, *J. Electrochem. Soc.* 127 (1980) 869.
- [17] M.Z. Kazacos, B. Miller, *J. Electrochem. Soc.* 127 (1980) 2378.
- [18] I. Nandhakumar, J.M. Elliott, G.S. Attard, *Chem. Mater.* 13 (2001) 3840.
- [19] B.M. Huang, T.E. Lister, J.L. Stickney, *Surf. Sci.* 392 (1997) 27.
- [20] C. Wei, N. Myung, K. Rajeshwar, *J. Electroanal. Chem.* 375 (1994) 109.
- [21] M.C. Santos, S.A.S. Machado, *J. Electroanal. Chem.* 567 (2004) 203.
- [22] M.O. Solaliendres, A. Manzoli, G.R. Salazar-Banda, K.I.B. Equiluz, S.T. Tanimoto, S.A.S. Machado, *J. Solid State Electrochem.* 12 (2008) 679.
- [23] S. Trasatti, O.A. Petrii, *J. Electroanal. Chem.* 327 (1992) 352.
- [24] M. Tian, G. Pell, B.E. Conway, *Electrochim. Acta* 48 (2003) 2675.
- [25] R.W. Andrews, D.C. Johnson, *Anal. Chem.* 47 (1975) 294.
- [26] T.E. Lister, J.L. Stickney, *J. Phys. Chem.* 100 (1996) 19568.
- [27] B.M. Huang, T.E. Lister, J.L. Stickney, *Surf. Sci.* 392 (1997) 27.
- [28] N. Furuya, S. Motoo, *J. Electroanal. Chem.* 102 (1979) 155.
- [29] M. Alanyalioglu, U. Demir, C. Shannon, *J. Electroanal. Chem.* 561 (2004) 21.
- [30] N. van Ngaç, O. Vittori, G. Quarini, *J. Electroanal. Chem.* 167 (1984) 227.
- [31] M. Volaire, O. Vittori, M. Porthault, *Anal. Chim. Acta* 71 (1974) 185.
- [32] A. Manzoli, S.A.S. Machado, *Thin Solid Films* 515 (2007) 6860.
- [33] A. Bănică, A. Culețu, F.G. Bănică, *J. Electroanal. Chem.* 599 (2007) 100.
- [34] Z. Fijaek, A. Lozak, K. Sarna, *J. Electroanal. Chem.* 10 (1998) 846.
- [35] M. Kemell, H. Saloniemi, M. Ritala, M. Leskelä, *Electrochim. Acta* 45 (2000) 3737.
- [36] R.W. Andrews, D.C. Johnson, *Anal. Chem.* 48 (1976) 1056.
- [37] M.F. Cabral, Ph.D. Thesis, University of São Paulo, 2008.
- [38] F. Sittner, W. Ensinger, *Thin Solid Films* 515 (2007) 4559.
- [39] E.A. Streltsov, S.K. Poznyak, N.P. Osipovich, *J. Electroanal. Chem.* 518 (2002) 103.
- [40] N. Furuya, S. Motoo, *Mater. Chem. Phys.* 22 (1989) 309.
- [41] B.W. Gregory, J.L. Stckiney, *J. Electroanal. Chem.* 300 (1991) 543.
- [42] M.F. Cabral, H.B. Suffredini, V.A. Pedrosa, S.T. Tanimoto, S.A.S. Machado, *Appl. Surf. Sci.* 254 (2008) 5612.
- [43] D. Lowinsohn, E.M. Ritcher, L. Angnes, M. Bertotti, *Electroanalysis* 18 (2006) 89.